Chapter 2
A Camera-Based Experimental Method for Mechanical Test on Patellar Tendons

Lorenzo Scalise, Barbara Lonzi, and Natascia Bernacchia

Abstract Tendons have an important structural function in biological systems, their mechanical proprieties are therefore of great interest in biomechanics engineering and reconstructive medicine. Their physiological characteristics require the study of specific experimental methods able to determine the mechanical properties.

In this work the authors propose a non-contact experimental method aimed to the characterization of the mechanical proprieties of rabbit patellar tendons based on the use of a single camera and a customized gripping system. The tensile test setup makes use of a fixed lens camera and a customized algorithm, providing the measurement of the local sample strain on different part along the tendon and of the cross-sectional area. The tensile stress is estimated by the value of the applied load and of the cross-section value of the sample; tensile stress values are calculated at a frequency of 8 Hz. Moreover a special design of the clamps and the use of the camera allow to protect the experimental tests from the well-known problem of peak force concentrations on the sample and slipping at its extremities, which indeed are typical problems in tensile testing of tendons.

Keywords Rabbit patellar tendons • Tensile test • Image analysis • Cross-sectional area • Gripping system

2.1 Introduction

Patellar tendon failure is a relatively rare lesion caused by forced flexion of the knee against an eccentric contraction of the quadriceps. This pathology could occur also in patients with systemic diseases that attack the soft tissue, such as rheumatoid arthritis [1]. Today the failure of patellar tendon is a very interesting and studied theme, because the tendon represents an important resource for autologous reconstruction of the cruciate ligament. This aspect becomes important especially in the sport medicine, where the incidence of the cruciate ligament injuries is particularly high [2].

Mechanical testing is frequently used to characterize tendons, and to analyze the effects of therapies and surgical interventions on their mechanical properties. Tendon physiological characteristics have been therefore already studied in the past years; such studies highlight the necessity to use specifically developed experimental methods to determine the mechanical properties.

The most reliable mechanical data were obtained by applying a tensile load on samples provided by both the insertions. A typical stress–strain curve for collagen-rich tissue, as the tendon, is non-linear and has an initial phase, when the crimps stretch out, called toe region [3], characterized by a large increase in the length with increasing force. When load increases, stiffness of the tissue also increases and progressively the curve is characterized by a sudden rise in the slope. The slope of this linear region is calculated as the value of Young's (or elastic) modulus of the tendon [3]. In literature different values for ultimate stress can be found, it varies from 28 to 44 N/mm^2 for young humans (with a strain to failure of 14–18 %). For tendons belonging to adult subjects, however, the ultimate stress varies between 42.5 and 113 N/mm^2 (with an elongation of 10–12.5 %) [4]. Elastic modulus in adult vertebrate varies from 0.8 to 2 GPa [5].

L. Scalise (✉) • B. Lonzi • N. Bernacchia
Dipartimento di Ingegneria Industriale e Scienze Matematiche (DIISM), Università Politecnica delle Marche,
Via Brecce Bianche 1, 60131 Ancona, Italy
e-mail: l.scalise@univpm.it

Due to their morphology and composition, in most of the cases, the gripping action of tendon samples for tensile can lead to a possible alteration of their mechanical characteristics, especially at their extremities where a cross-section reduction occurs. Clamping the tendon into a test machine is a known major problem, which derives from the independence of the fibrous units, that has to be separately held, therefore a technique such as gluing, which holds only the outside of the tendon, is not fully appropriate [5]. Gripping directly the specimen between two metal plates determines a serious distortion of the fibers, with consequent non-uniform concentrations of load and deformation, resulting in premature failure. Another problem could be possible slippage respect to the grips, due to the low friction coefficient. In literature it is possible to find several solution aiming to solve the problem of clamping tendons [5], unfortunately none of them completely solves all the problems. Riemersa and Schamhardt [6] have described the "cryo-jaw", a cooled clamp with liquid carbon dioxide (CO_2), with plates provided by channels for tissue freezing. Since then, cooled terminals were considered the gold standard for the mechanical tests with high applied loads on the soft tissues. It should be emphasized that the cryogenic techniques [7, 8] create a zone of thermal transition, which may alter the mechanical properties of the tendon tissue. The possibility to incorporate tendon extremities in resin was evaluated, in order to avoid the problem of stress concentration at the ends of the sample [9].

A second relevant aspect is related to the need to carefully estimate the geometric characteristics of the tendon [10] in order to determinate the mechanical properties of tendons. Legerlotz et al. found that specimen length and cross-sectional area (CSA) appear to influence failure stress, strain and modulus in fascicles from two functionally different tendons [11]. Measurement of the previous mentioned geometrical parameters is really important to correctly assess tendon mechanical behavior. Goodship et al. [12] summarized the main methods historically used to measure CSA. The first technique is based on cutting sections of the tendon, although it allows morphological measurements, it is destructive and mechanical tests cannot be performed subsequently. Other research group thought to acquire tendon dimensions using a microscope. To allow measurement of CSA in structures with a non-uniform shape, a device known as an area micrometer was developed; in order to adopt this technique, it is necessary to compress the tendon into a rectangular slot of known width until the tendon completely fills the slot. However, this technique is affected by the applied pressure and permanent damage could occur to the soft tissue. In 1996 Race and Amis adopted a technique to measure tendon CSA by making a silicone rubber cast and a mold of the structure. The drawbacks of this technique are that it is time consuming, dehydration and shrinkage of the sample.

Due to the tendon nature of soft tissue, contact could alter shape and real cross-section. The need of no contact technique and systems able to provide the measurement of strain and sample CSA, is clear. Some authors [13,15] developed a method based on measuring the width of the tendon using incremental degrees and then calculating the CSA by integration. Recently an optical approach has been proposed [13], consisting on laser light projection perpendicular to the sample axis, digital camera acquisition of the scene and image processing. Despite the high resolution and precision achievable, the testing time is still limiting its use in dynamic and fatigue testing, due to the need to stop and restart the test to allow the previous described task. An assessment of tendon biomechanics and its relation with age was conducted [14] on rabbit patellar tendons. In this work cross-section was measured in three equidistant locations with a camera and the averaged value was calculated. Revel et al. [15] conducted a study on vibrational properties of rabbit Achilles tendons where their length was measured using a video dimensions analyzer (VDA), which has also the role to monitor any slippage. Limitations can be found in the complexity of these techniques and in the possibility to measure cross-sections at fixed intervals only stopping and restarting the test.

In this work, a novel non-contact measurement method is proposed for the characterization of the mechanical proprieties of rabbit patellar tendons based on the use of a single camera and a customized gripping system. The tensile test setup makes use of a fixed lens camera, measuring the local sample strain simultaneously along the tendon length and cross-sectional area frame by frame. The experimental setup will be validated and the choice of the rabbit as an experimental animal model was suggested by the similarity of its extensor mechanism with the human one.

## 2.2 Experimental Set Up and Measurement Procedure

The aim here is to propose the design of a new measurement bench for mechanical characterization of biological materials, in details rabbit patellar tendons, to allow tensile tests, using some traditional instrumentation but also new strategies to solve main problems connected with biological tissues, like sample clamping and assessing the real elongation and cross-section of the sample.

The apparatus is composed by a clamping system, a servo-pneumatic uniaxial test machine and a data acquisition unit, a PC, a non-contact strain measurement system and an illumination source (Fig. 2.1).

Fig. 2.1 Experimental setup
scheme for tensile tests
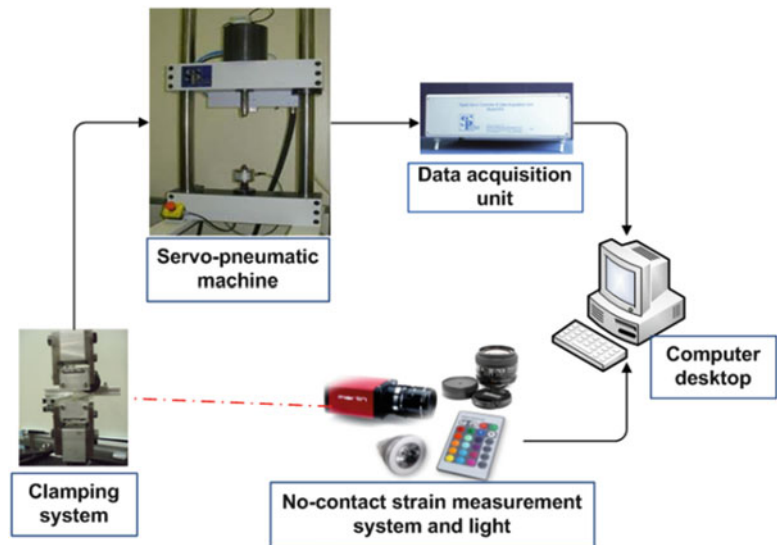
Fig. 2.2 Clamping system
design and realization
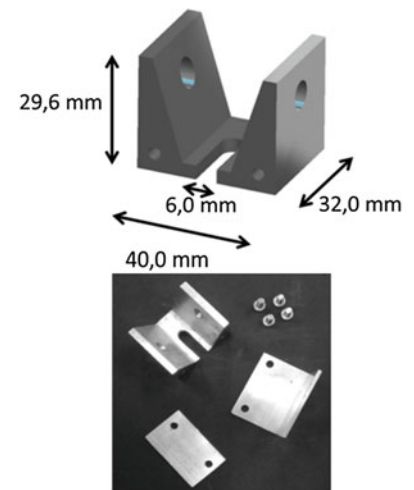
The experimental setup has been firstly tested on reference material with known mechanical behavior. In particular Nylon 6 wires (with diameter of 0.7 mm) were chosen. To this aim the international standard UNI EN ISO 527-1/1997 [16] was taken in consideration for test procedure and to compare stress–strain curves obtained with the experimental setup. In the following all the components will be discussed, highlighting the proposed solutions.

An appropriate clamping system has been studied in order to optimize sample gripping without modifying its mechanical properties and avoiding its slippage. Technical requirements were defined analyzing dimensions of the sample, with a well-documented study in literature [17]. A length of 17.2 ± 1.5 mm and a CSA of 13.3 ± 1.0 mm^2 were found. For what concerns the gripping technique both cryogenic method and mechanical serration were discarded due to the possibility to create a damage at tendon ends and alter its mechanical behavior, especially because rabbit patellar tendon are small structures. The choice was done considering the inclusion of tendon ends in cement inside custom designed clamps. In Fig. 2.2 the innovative clamping system could be seen in all its components; it has been realized in aluminium and appropriately studied to withstand and distribute tension, avoiding failure also using plates fixed with screws. An holding system allows to connect the grips with the testing machine, and an angular bar serves to maintain the correct alignment of the sample during each phase of the preparation procedure.

Tensile tests were carried out using a Servo-pneumatic test machine 966-804-23 made (Si-Plan Electronics Research Ltd$^©$) provided by an actuator rod, with embedded displacement transducers (maximum stroke equal to 50 mm), and a load cell (maximum calibrated force: 2 kN). The equipment includes also a data acquisition unit and a manufacturer software, which works with the operating system Windows XP$^®$, characterized by an extremely simple interface that allows the user to enter test settings and, at the same time, to observe in real time quantities of interest. In this work the tests were performed in

Fig. 2.3 AVT Marlin F-131
camera and optical zoom

Table 2.1 Camera settings

Brightness (relative)	50
Gain	7
Shutter (relative)	4,095
Lens opening	2.8
Focus	0.3

displacement control mode. Moreover it is possible to choose sample frequency, ramp rate, maximum and minimum values, waveform, cycles number, etc.

As reported in the introduction, we aimed to be design and experimental system able to observe eventual gliding during the application of the tensile load. To this aim, the measurement of the sample strain was determined processing images captured during the test by a digital camera with fixed lens. A Marlin F-131 camera (Allied Vision Technologies, Fig. 2.3) was used, with a IEEE 1394 firewire connection (field of view: 1,280 × 1,204 pixels). Camera settings, as sample frequency, brightness, gain and shutter, can be selected through Measurement and Automation software (National Instruments). Considering the small size of the rabbit patellar tendons, in order to improve image resolution, that is to reduce the pixel size, an AF NIKKOR 24 mm 1: 2.8 D optical zoom was added. Technical settings of the camera (Table 2.1) affect the value of the sampling frequency. For all our tests, a sampling frequency of 8 Hz (or fps, frame per second) was used, while a sampling frequency of 80 Hz was used for displacement and force signals generated by the test machine.

The camera was placed perpendicularly to the clamping system at a distance of 20 cm from the sample. In order to enhance the image contrast, a white led light source and a black background screen were used. From camera calibration with 3 gauge blocks [18] ($\dim_{mm}1 = 3.415$ mm, $\dim_{mm}2 = 2.935$ mm and $\dim_{mm}3 = 4.005$ mm), pixel size was determined using the following equation:

$$pixel\ size_{(mm)} = \frac{\dim_{mm}}{\dim_{pixel}} \tag{2.1}$$

Camera calibration was done recording the support placed in specimen test plane. Images were analyzed with a custom algorithm realized in Matlab$^{\circledR}$ (Mathworks) environment, to measure $\dim_{pixel}$, i.e. block dimension in pixels.

2.3 Materials and Methods

Ten patellar tendons were extracted from five healthy rabbits, 3–4 months old (3.5 ± 0.5 kg), and maintained in low saline solution at $-20\ ^\circ$C until the test day [15, 19]. The protocol was the same for all the samples, consisting in dissection of the tendon from muscle tissue, keeping the patella in the upper side and the tibial bone insertion in the lower side. Before tensile tests, specimens were thawed for 4 h at room temperature ($20\ ^\circ$C) covered with a sterile gauze soaked with physiological saline solution, in order to avoid dehydration. The tendon was gripped with the innovative clamping system described previously. First a silicone spray was applied in order to easily clean the clamps after the experiment. After that both the ends of the sample, patella and tibial insertion, have been embedded in a synthetic resin inside the clamps (Fig. 2.4), taking care in preventing sample drying using physiological saline solution. On the central area of tendon two markers were created, at a distance of 4 mm from the clamps, using black ink. In this work all the tests were performed in displacement control mode, in order to check actuator movement through parameters like maximum and minimum values, ramp rate, expressed respectively in mm and mm/s. Load and displacement data were saved in CSV format (Comma Separated Value). The image sequences were acquired during the tests using a custom interface implemented in LabView$^{\circledR}$ (National Instruments)

Fig. 2.4 Tendon assembly
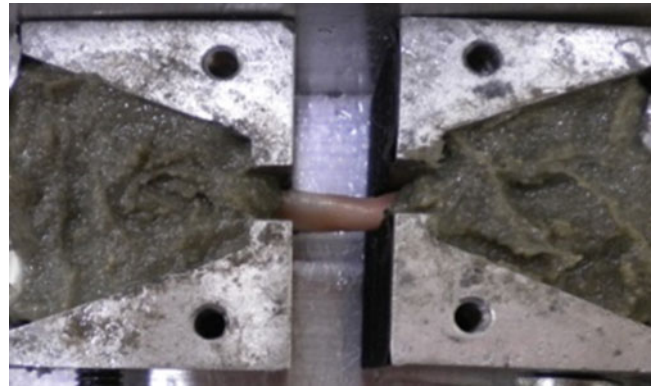
environment, allowing to start and stop the acquisition, finally to save images in bmp format (bitmap). A trigger has been used to synchronize data acquisition from camera and tensile test start.

After sample preparation and assembly on test machine, a caliper (resolution of 0.05 mm) was used to measure l_0 (initial length) as the distance between the clamps. Rabbit patellar tendons were preloaded applying a constant elongation equal to 1 % l_0 for 10 min [20]. After that sample was subjected to a preconditioning procedure performing 10 loading-unloading cycles with a deformation varying between 0 and 2 % l_0. It is possible to notice that this range corresponds to the initial toe region, that typically characterize tendon stress–strain curve [3], in which all the fibers are crimped, so this step is essential for their straightening before the tensile test. For tendon an elongation rate of 0.3 mm/s [21] was chosen due to its viscoelastic nature. Last step was constituted by the tensile test performed at the same rate of the previous phase.

A custom algorithm was developed in Matlab$^{®}$ environment to analyse acquired data. The processing was divided into two parts due to the nature of information: machine data and image sequences, stored respectively in comma separated value format (.csv) and bitmap (.bmp). Preliminary the off-set compensation is operated on the initial values from the load cell and the testing machine displacement transducer. Load signal was low-pass filtered with a II order Butterworth filter with a normalized cut-off frequency of 0.03 Hz. Considering displacement signal as Δl, longitudinal tensile strain ε_l was determined at any time instant as the elongation Δl divided by the initial length l_0 [16]:

$$\varepsilon_l = \frac{\Delta l}{l_o} \tag{2.2}$$

Unitary tensile stress σ was calculated as the ratio between load to which the sample is subjected and its initial cross-sectional area (CSA) [16].

$$\sigma = \frac{F}{CSA} \tag{2.3}$$

Tendon CSA was calculated from the first frame with segmentation technique, multiplying the number of white pixels counted on a chosen line in the central area of the specimen, by the pixel size. Cross-sectional area was found as $(d/2)^2 \pi$, assuming a circular model for the tendon section area [22]. From the stress–strain curves the following parameters were determined: ultimate tensile strength and ultimate strain (σ_u, ε_u), Young modulus (E). The last is usually evaluated using linear regression analysis as it is reported in [16] for reference specimens, but for tendons it was necessary to calculate Young modulus as the slope in the linear region of the stress–strain curve that is the portion which presents a deformation between 2 and 4 %, as it is also reported in [3]. The equation used for the calculation of E is:

$$E = \frac{\sigma_2 - \sigma_1}{\varepsilon_2 - \varepsilon_1} \tag{2.4}$$

What we can obtained from these curves are nominal values of analyzed mechanical properties. In order to compare tensile test curves with image-derived deformation it is necessary to resample load cell signal. As regards image sequences, a region of interest was chosen on the last frame of the test, when the complete actuator stroke is reached. The ROI is constituted by specimen location and both the clamping system and the markers should be clearly visible, so it was selected also taking the lower reference line. Subsequent processing was done only on this region that was selected for all the test frames. Image processing began with a contrast enhancement. After that, images were converted from grayscale to binary
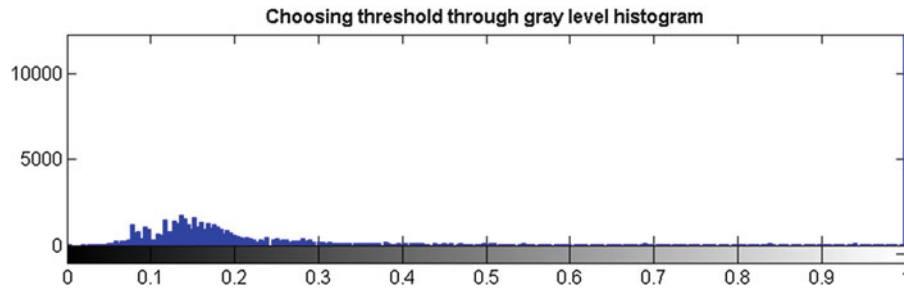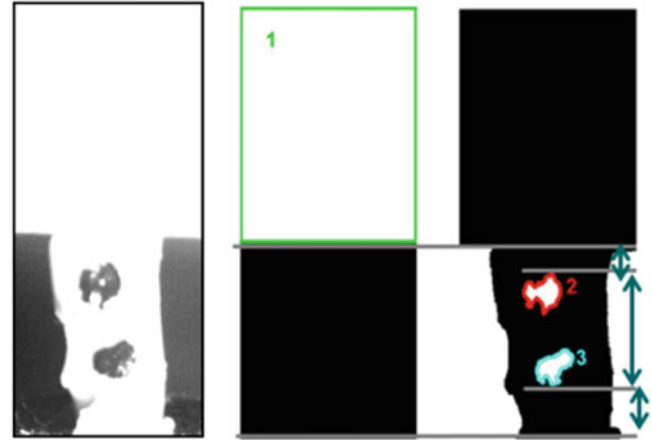
Fig. 2.5 Gray level histogram

Fig. 2.6 Image segmentation

coding in order to obtain black and white ones, using a threshold that could be chosen by the user, looking at gray level histogram (Fig. 2.5). The threshold was not fixed for all the samples, due to the variability of natural illumination during the test days, despite the fact that the test room is pretty isolated by the external ambient. The tendon makes segmentation process difficult cause of its gray level is similar to that of the clamp. However targets are dark, in contrast to those applied on the wire. In particular images were treated with opening, a morphological operation that allows sample removal in order to see the upper clamp, using a line as sliding structure. Complementary images were computed from those ones just converted in binary format, in which it is possible to correctly identify white objects with an edge-based segmentation algorithm. The reference line on the lower clamp was fixed, instead of the upper one and the markers that move during the test and in some cases could not be well recognized. To address this problem they were automatically localized for each frame implementing a procedure that assesses the distance of each target respect to the position in the previous frame and searching the minimum value. In this way, locations of the markers and upper clamp were determined considering maximum or minimum height as it can be seen in Fig. 2.6.

Distances between the two markers were computed and converted in mm in order to obtain the length l; the longitudinal strain ε_l was measured using:

$$\varepsilon_l(t) = \frac{l(t) - l_0}{l_0} \tag{2.5}$$

where l_0 is the sample initial length measured from the first frame. Moreover through image analysis it was possible to measure the sample diameter for each frame, allowing to have a continuous CSA measurement during the test. In this way stress values can be calculated as:

$$\sigma(t) = \frac{F(t)}{CSA(t)} \tag{2.6}$$

All mechanical parameters were found, as it was previous discussed for nominal curves, but using strain and cross-section measurements provided by image analysis.

2.4   Experimental Results

Data measured with the camera-based measurement method was validated considering, as reference method, data measured with the displacement and force sensors of the tensile test transducer; validation tests were performed on nylon samples. From scatter-plot of the measured data, a Pearson squared correlation coefficient $R^2 = 0.99$ was obtained and the extended uncertainty of the strain measurement, calculated according [23], was:

$$U_\varepsilon = \sqrt{\left(\frac{\partial f}{\partial x_1} \cdot u_{x_1}\right)^2 + \left(\frac{\partial f}{\partial x_2} \cdot u_{x_2}\right)^2} \tag{2.7}$$

where $x_1 = \Delta l$, $x_2 = l_0$, and $\varepsilon = f(\Delta l, l_0)$.

A value of 0.03 was obtained as extended uncertainty on strain measurement, considering a confidence interval with a coverage factor $k = 1$.

Rabbit patellar tendons were preconditioned applying an elongation in the range of 2–4 %, in order to allow fibers stretching and uncrimping. Loading/unloading cycles (N = 10) were analyzed and it was possible to notice that the stress/strain curve is shifted to the right along the X axis in each load cycle, revealing the presence of a non-elastic and hysteretic behavior as it was found in literature [24]. In Fig. 2.7 stress/strain curve of quasi-static tensile tests are visible. The upper curve was obtained using data provided by the sensors of the tensile test machine and considering single CSA (calculated from the first video frame); the lower curve instead reports the stress/strain curve simultaneously measured with the proposed measurement method where CSA and strain measurements were obtained with the proposed image-based method. Both the curves show a curve trend comparable with that showed in literature [3], but the slipping of one of the sample extremity is detectable in the later (Fig. 2.8).

Transverse strain was also evaluated from the frames and it is reported in Fig. 2.9, showing the necking of the sample during the tensile test. In the following figures (Figs. 2.10, 2.11 and 2.12) box-plots of Young modulus, ultimate strain and ultimate strength are finally presented.
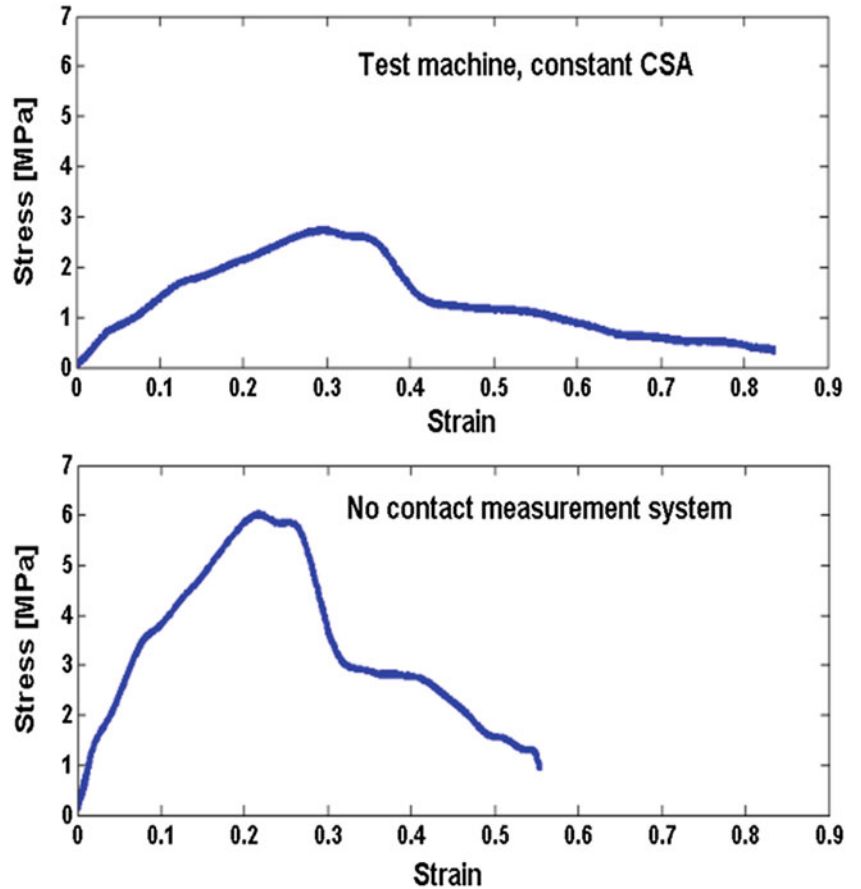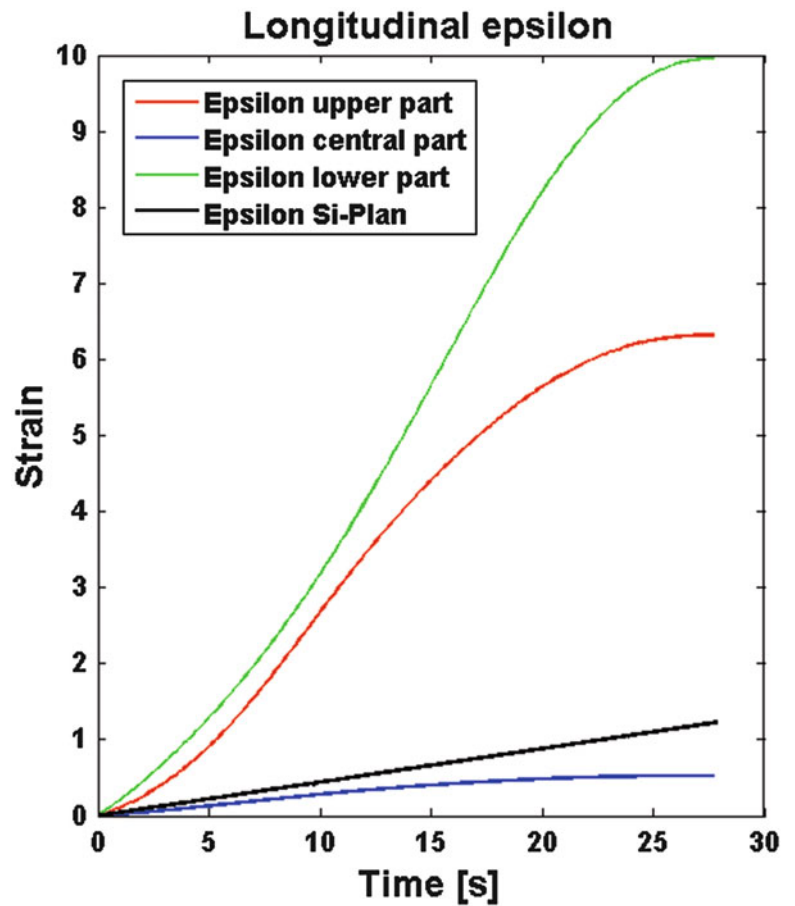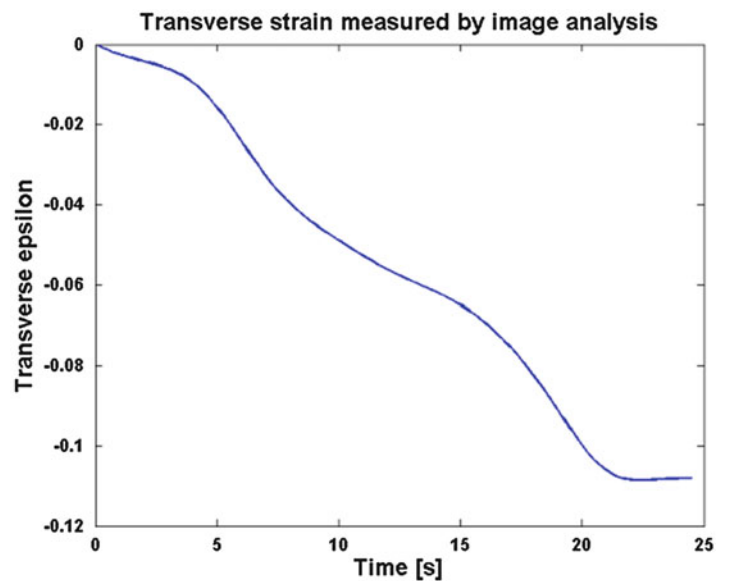

Fig. 2.7 Example of a stress/strain curve of rabbit patellar tendon

Fig. 2.8 Strain measured
by machine and camera
(in the three segments)


Fig. 2.9 Transverse strain

In Fig. 2.10, the Young's modulus is calculated using the data obtained by the tensile machine (Machine), the data from the new proposed method for the evaluation of strain but a constant cross-section area (Camera) and final the strain and the cross-section area evaluated with the image-system (Variable CSA).

In Figs. 2.11 and 2.12, the ultimate strain and stress are calculated using the data obtained with the tensile machine (Test Machine) and the data from the new proposed method (strain and CSA measurement frame-by-frame) (Camera).
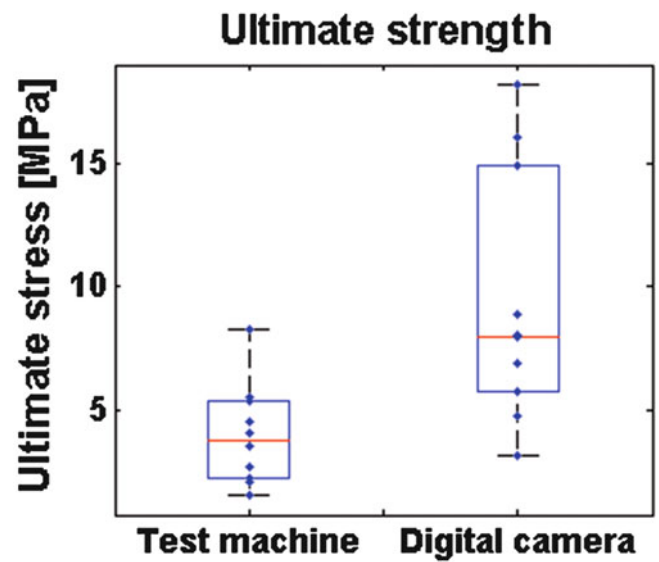
Fig. 2.10 Boxplot of Young modulus
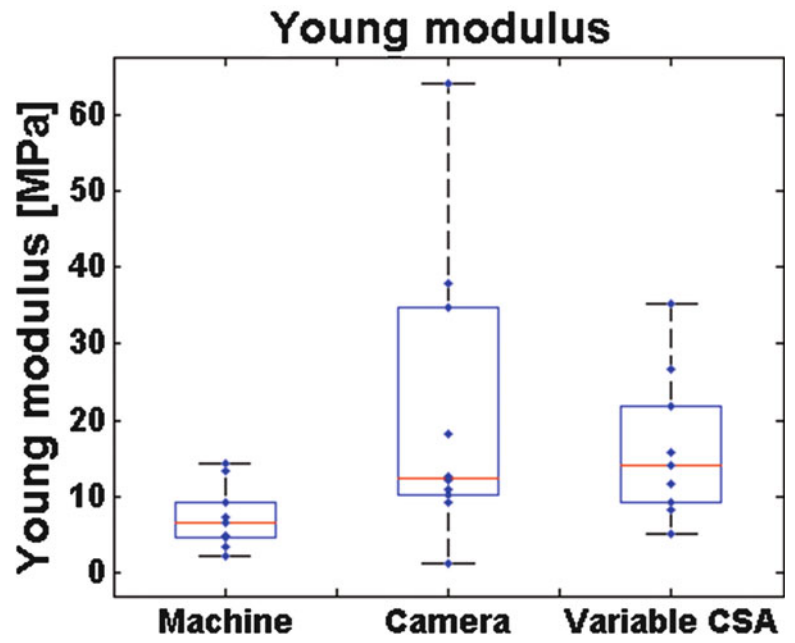
Fig. 2.11 Boxplot of ultimate strain
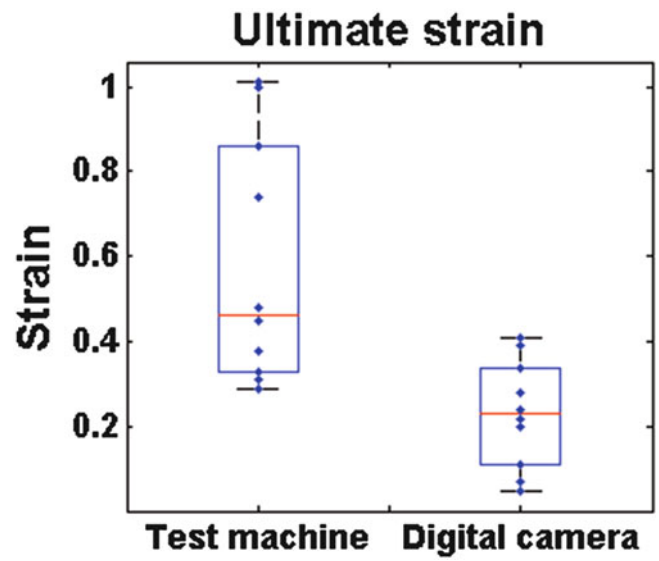
Fig. 2.12 Boxplot of ultimate strength

2.5   Conclusions

The new measurement method is based on the digital image processing, using techniques as filtering, segmentation, edge detection. These tools are powerful in order to measure longitudinal strain and CSA completely contactless, obtaining results that fit well to the values found literature. The proposed method was validated using samples of known mechanical characteristics (nylon) showing a good correlation ($R^2 = 0.99$) and an extended uncertainty on strain measurement rather limited (0.03).

One of the innovative aspects of the proposed method lies in the fact that the image analysis should provide a local measure of the strain which allows the control and correction of slipping phenomena. Also important it is the frame-by-frame measurement of the sample cross-sectional area. It should be noted that the majority of methods reported in the literature is based either on destructive methods (such as casts or insertion into preformed frames) or on optical methods (such as laser, or use in conjunction with a video dimension analyser) but they still do not guarantee a continuous measurement and often require to stop and restart the test, to be able to capture the sample.

Moreover tendons are considered to have a viscoelastic behavior, so it is essential to measure both the two quantities in order to correctly characterize and study mechanical parameters of this biological material. The experimental protocol developed in this work allowed to realize a suitable preconditioning of the tendon fibers, as can be observed by the decrease of the area inside the hysteresis loop, and at the same time it ensured a good performance in the tensile tests, correctly determining the sample rupture in its middle section.

Future steps in this work will be to study tendons in pathological conditions, in order to test the efficacy of grafts or therapies, and to design a new and custom clamping system also for samples of larger size. Another topic would be to validate the clinical evidence that the use of collagen I membranes in tendons could enhance and facilitate its repair. In particular a study on the behavior of tendons from the mechanical point of view could be realized to assess the changes resulting from the presence of the membrane.

From the experimental point-of-view the next improvement will aim to introduce a second camera, perpendicular to the optical axis of the first one, allowing to model the sample cross-section area with a ellipse [21].

References

1. Pritchard CH, Berney S (1989) Patellar tendon rupture in systemic lupus erythematosus. J Rheumatol 16(6):786–788
2. Alentorn-Geli E, Myer GD, Silvers HJ, Samitier G, Romero D, Lázaro-Haro C, Cugat R (2009) Prevention of non-contact anterior cruciate ligament injuries in soccer players. Part 1: mechanisms of injury and underlying risk factors. Knee Surg Sports Traumatol Arthrosc 17(7):705–729
3. Wang JH-C (2006) Mechanobiology of tendon. J Biomech 39:1563–1582
4. Ippolito E, Natali PG, Postacchini F, Accinni L, De Martino C (1980) Morphological, immunochemical and biochemical study of rabbit Achilles tendon at various ages. J Bone Joint Surg 62(4):583–592
5. Ker RF (2007) Mechanics of tendon, from an engineering perspective. Int J Fatigue 29(6):1001–1009
6. Riemersa DJ, Schamhardt HC (1982) The cryo-jaw, a clamp designed for in vitro rheology studies of horse digital flexor tendons. J Biomech 15(8):619–620
7. Sharkey NA, Smith TS, Lundmark DC (1995) Freeze clamping musculo-tendinous junctions for in vitro simulation of joint mechanics. J Biomech 28(5):631–635
8. Rincon L, Schatzmann L, Brunner P, Stäubli HU, Ferguson SJ, Oxland TR, Nolte LP (2001) Design and evaluation of a cryogenic soft tissue fixation device - load tolerances and thermal aspects. J Biomech 34(3):393–397
9. Shapiro PS, Rohde RS, Froimson MI, Lash RH, Postak P, Greenwald AS (2007) The effect of local corticosteroid or ketorolac exposure on histologic and biomechanical properties of rabbit tendon and cartilage. Am Assoc Hand Surg 2(4):165–172
10. Woo SL, Gomez MA, Sites TJ, Newton PO, Orlando CA, Akeson WH (1987) The biomechanical and morphological changes in the medial collateral ligaments of the rabbit after immobilization and remobilization. J Bone Joint Surg 69(8):1200–1211
11. Legerlotz K, Riley GP, Screen HR (2010) Specimen dimensions influence the measurement of material properties in tendon fascicles. J Biomech 43(12):2274–2280
12. Goodship AE, Birch HL (2005) Cross sectional area measurement of tendon and ligament in vitro: a simple, rapid non-destructive technique. J Biomech 38(3):605–608
13. Salisbury STS, Buckley CP, Zavatsky AB (2008) Image-based non-contact method to measure cross-sectional areas and shapes of tendons and ligaments. Meas Sci Technol 19(4):045705
14. Dressler MR, Butler DL, Wenstrup R, Awad HA, Smith F, Boivin GP (2002) A potential mechanism for age-related declines in patellar tendon biomechanics. J Orthop Res 20(6):1315–1322

15. Revel GM, Scalise A, Scalise L (2003) Measurement of stress–strain and vibrational properties of tendons. Meas Sci Technol 14(8):1427–1436
16. UNI EN ISO 527-1/1997 (1997) Plastics – determination of tensile properties
17. Maeda E, Tohyama H, Noguchi H, Yasuda K, Hayashi K (2010) Effects of maturation on the mechanical properties of regenerated and residual tissues in the rabbit patellar tendon after resection of its central one-third. Clin Biomech 25(9):953–958
18. UNI EN ISO 3650: 2002 (2002) Geometrical product specifications (GPS) - length standards - Gauge blocks
19. Woo SL, Orlando CA, Camp JF, Akeson WH (1986) Effects of postmortem storage by freezing on ligament tensile behavior. J Biomech 19(5):399–404
20. Fujie H, Yamamoto N, Murakami T, Hayashi K (2000) Effects of growth on the response of the rabbit patellar tendon to stress shielding: a biomechanical study. Clin Biomech 15(5):370–378
21. Ohno K, Yasuda K, Yamamoto N, Kaneda K, Hayashi K (1996) Biomechanical and histological changes in the patellar tendon after in situ freezing. Clin Biomech 11(4):207–213
22. Parent G, Cyr M, Desbiens-Blais F, Langelier E (2010) Bias and precision of algorithms in estimating the cross-sectional area of rat tail tendons. Meas Sci Technol 21(12):1–8
23. International Organization for Standardization (1993) Guide to the expression of uncertainty in measurement, 1st edn. International Organization for Standardization, Switzerland (corrected and reprinted 1995)
24. Woo SL, Debski RE, Zeminski J, Abramowitch SD, Saw SSC, Fenwick JA (2000) Injury and repair of ligaments and tendons. Annu Rev Biomed Eng 2:83–118